Isolation of Myotoxic Component From Rattlesnake (*Crotalus viridis viridis*) Venom

Electron Microscopic Analysis of Muscle Damage

Charlotte L. Ownby, MS, PhD, David Cameron, MS, and Anthony T. Tu, PhD

The pathogenesis of myonecrosis induced by a purified component of rattlesnake (*Crotalus viridis viridis*) venom was studied at the light and electron microscopic levels. Crude venom was fractionated by gel filtration (Sephadex G-50) followed by cation exchange chromatography (Sephadex C-25). Electrophoretic homogeneity of the isolated myotoxin (Fraction II from C-25 column) was demonstrated in isoelectric focusing and disc gel polyacrylamide gel electrophoresis. White mice were injected intramuscularly with 1.5 μg/g of the purified protein in 0.1 ml of physiologic saline. Light microscopic examination of injected muscle revealed a series of degenerative events including partial vacuolation of muscle cells at 6, 12, and 24 hours and complete vacuolation and loss of striations at 48 and 72 hours. Hemorrhage was not observed. At the electron microscopic level the perinuclear space and sarcoplasmic reticulum were dilatated in all samples. By 48 and 72 hours the myofibrils lacked striations and the sarcomeres were disorganized. Plasma membranes and T tubules remained intact in all samples. These results correlated well with the myonecrosis induced by crude *Crotalus viridis viridis* venom except for several important aspects. The pure component altered skeletal muscle cells specifically, with the sarcoplasmic reticulum being the primary site of action. (Am J Pathol 85:149–166, 1976)

SNAKEBITE POISONING is a serious medical problem throughout the world. It has been estimated that there are 30,000 to 40,000 deaths each year due to the bite of venomous snakes.[1] In the United States the incidence of snakebite is lower, yet, 188 people died as a result of the bites of venomous snakes in a 9-year period (1950–1959); 20% of these bites were due to rattlesnakes.[2] In 1968 the Department of the Navy recorded 700 to 1000 bites resulting in about 20 deaths, all due to rattlesnakes.[3] The widespread use of commercially available antivenin probably accounts for the low mortality rate of snakebite victims in the United States. However, antivenin may not prevent local tissue damage such as hemorrhage and myonecrosis,[4-6] which in many cases leads to dysfunction or complete loss of an extremity. Thus, in the United States today, the main health problem resulting from snakebite poisoning is local tissue damage, i.e., hemorrhage and myonecrosis.

From the Department of Physiological Sciences, Oklahoma State University, Stillwater, Oklahoma, and the Department of Biochemistry, Colorado State University, Fort Collins, Colorado.

Supported by Grant 5R01 GM-15591 from the National Institutes of Health.

Accepted for publication June 1, 1976.

Address reprint requests to Dr. Anthony T. Tu, Department of Biochemistry, Colorado State University, Fort Collins, CO 80523.

The pathogenesis of hemorrhage induced by rattlesnake venom has been investigated at both light and electron microscopic levels.[7] The pathogenesis of myonecrosis induced by rattlesnake venom has also been investigated at the light [8] and electron microscopic [9] levels. These studies were made on crude rattlesnake venom; thus, the effects may be due to one component, a combination of several, or all of the components present in crude venom. Myotoxic components have been isolated from at least one snake venom. Two myonecrosis producing factors were identified in habu (*Trimeresurus flavoviridis*) venom—one heat-stable, the other heat-labile.[10] The purpose of the present investigation was to isolate the myotoxic component of *Crotalus viridis viridis* venom and to use it to study the pathogenesis of muscle damage with the electron microscope.

Materials and Methods

Fractionation of Venom

Crude prairie rattlesnake (*Crotalus v. viridis*) venom in lyophilized form, purchased from Miami Serpentarium Laboratories, was subjected to initial fractionation by gel filtration on a Sephadex G-50 column (2.5 cm × 45 cm). A sample of crude venom was dissolved in 3 to 4 ml of an elution buffer composed of 0.05 M Tris buffer (pH 9.0 at 21 C) and 0.1 M KCl. The column was developed with this elution buffer at a flow rate of 30 ml/hr. Eluate absorbance at 280 nm was monitored with an ISCO UV column monitor. Tubes were pooled as indicated and the amount of protein in each pooled fraction was determined by the method described by Lowry *et al.*[11]

Gel filtration fraction G-50 III was further fractionated by cation exchange chromatography on a C-25 (CM Sephadex) column (1 cm × 15 cm). The C-25 column was equilibrated with the elution buffer used with the G-50 column. The column was developed with a stepwise KCl salt gradient in the 0.05 M Tris buffer. Absorbance of the eluate at 280 nm was again monitored.

Fractions were desalted by dialysis or by passage through a Sephadex G-10 column. Desalted fractions were lyophilized and stored at below 0 C.

Assay for Myotoxic Activity During Fractionation

All mice used in a light microscope assay for muscle damaging activity were from a conventional colony of Swiss Webster white mice which has been maintained by random breeding of mice originally purchased from CAMM Research Institute. Mice weighing 30 to 35 g were injected in the medial aspect of the thigh with 0.1 ml of 0.9% NaCl containing 50 μg of the fraction to be assayed. Mice were sacrificed by cervical dislocation from 24 to 72 hours following injection, and an approximately cubical tissue sample, 4 or 5 mm on a side, was removed from the back of the thigh. Tissue samples were fixed for 16 hours at room temperature in Bouin's fixative, washed, dehydrated, and embedded in paraffin. Sections were stained with hematoxylin and eosin for light microscope examination.

Demonstration of Protein Homogeneity

Isoelectric focusing polyacrylamide gel electrophoresis was done in gels over the pH range 3.5 to 10 using ampholytes purchased from LKB Instruments, Inc. Focusing was done in 7.5% gels at 100 V for 1 hour, then at 200 V for 4 hours. Protein was fixed and ampholytes removed by soaking in 20% tricholoroacetic acid (TCA), or in 20% TCA

containing 10 mM $HgCl_2$ for a period of 48 hours, following which the gels were stained with 0.05% Coomassie blue in 19% TCA.

Disc polyacrylamide gel electrophoresis was done in the β-alanine system.[12] Components of the system were prepared as follows: *upper reservoir buffer*—3.55 g β-alanine + 2.37 ml HOAc + H_2O to 1 liter. *lower reservoir buffer*—50 ml 1.0 N NaOH + 3.66 ml HOAc + H_2O to 1 liter. *stacking gel*—2 volumes 5% acrylamide, 1.25% methylenebisacrylamide, 1 volume 0.188 M NaOH containing 1.08 ml HOAc and 0.1 ml tetramethylethylene diamine (TEMED) per 100 ml, 1 volume 0.002% riboflavin. *resolving gel*—1 volume 20% acrylamide, 0.8% methylenebisacrylamide, 1 volume 0.185 M NaOH containing 3.44 ml HOAc and 0.2 ml TEMED per 100 ml, 2 volumes 0.1% ammonium persulfate. Following electrophoresis, gels were stained with 0.05% Coomassie blue in 19% TCA.

Electron Microscopy

The purified, lyophilized myotoxic fraction obtained from the Sephadex C-25 column was dissolved in 0.85% physiologic saline (PSS). Experimental mice were injected with 1.5 μg g of the fraction in 0.1 ml of PSS; control mice were injected with 0.1 ml of 0.85% PSS. All mice were injected intramuscularly in the lateral aspect of the right thigh (biceps femoris muscle). The mice were killed by cervical dislocation at 3, 6, 12, 24, 48, and 72 hours after the injection of myotoxic fraction or PSS. Twenty-seven white mice weighing 18 to 20 g were used. Muscle was taken from the medial aspect of the injected thigh (gracilis and semimembranous muscles) to avoid sampling regions damaged by the needle.

The tissue was fixed initially in 2% glutaraldehyde in cacodylate buffer (pH 7.4) for 2 hours at 4 C. After rinsing in cacodylate buffer for 12 to 18 hours at 4 C, the tissue was postfixed in 2% osmium tetroxide in cacodylate buffer (pH 7.4) for 1 hour at 4 C. Dehydration through a graded series of ethanol was followed by embeddment in DER 332-732 [13] in flat embedding molds. Thick sections (0.5 to 1.0 μ) were cut on a Sorvall MT-2 ultramicrotome, stained with toluidine blue,[14] and examined with the light microscope for damaged fibers. Silver and silver-gray sections were cut with a Sorvall MT-2 ultramicrotome using glass knives and mounted on uncoated and unsupported copper grids. Sections were stained with aqueous uranyl acetate and lead citrate,[15] then observed and photographed with a Philips EM 200 electron microscope.

Results

Isolation of Myotoxic Factor

Five protein fractions, as shown in Text-figure 1, were obtained from the G-50 gel filtration. Total protein in the pooled tubes was distributed among the G-50 fractions as follows: I, 20%; II, 44%; III, 21%; IV, 9%; and V, 6%. G-50 III was found by the light microscope assay to have strong myotoxic activity and was further fractionated by C-25 cation exchange chromatography to give two protein fractions, as shown in Text-figure 2. Assay showed no apparent myotoxic activity in fraction C-25 I, with the total myotoxic activity present in C-25 II. The protein in C-25 II was shown to be highly purified by its electrophoretic homogeneity in both isoelectric focusing and β-alanine disc gel electrophoresis. As shown in Figure 1, fixation of the C-25 II protein by 20% TCA was enhanced by addition of 10 mM $HgCl_2$ to the TCA.

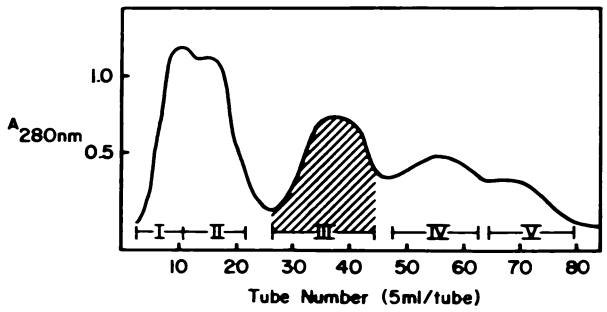

TEXT-FIGURE 1—Elution profile of crude venom on G-50 gel filtration column. Crude venom was dissolved in elution buffer composed of 0.05 M Tris buffer (pH 9.0 at 21 C) and 0.1 M KCl and applied to the column. The column was washed with the same elution buffer. Fraction III (*hatched area*) was found to have myotoxic activity and was subjected to cation exchange step.

Electron Microscopy

Control Muscle

Muscle from control animals was normal in all aspects. Gross examination of the muscle revealed no lesions. Light microscopic examination of thick (1 μ) sections revealed the typical histologic organization of skeletal muscle. The muscle fibers (cells) were grouped into fascicles; the connective tissue layers were typical and did not contain evidence of hemorrhage or edema. The fibers themselves were intact. Electron microscopic examination of thin sections revealed the typical fine structural organization of skeletal muscle (Figure 2). Transverse and longitudinal striations were prominent and consisted of the A and I bands and the thick and thin filaments, respectively. In longitudinal sections of muscle the A band, H band, I band, M lines, and Z lines were visible and typical. At the junction of the A and I bands, triads were observed which consisted of two dilated terminal cisterns of the sarcoplasmic reticulum and one T tubule (Figure 3). The remainder of the sarcoplasmic reticulum consisted of typically flattened cisterns. Mitochondria were located between the myofibrils, beneath the sarcolemma, and at the poles of the nuclei. The

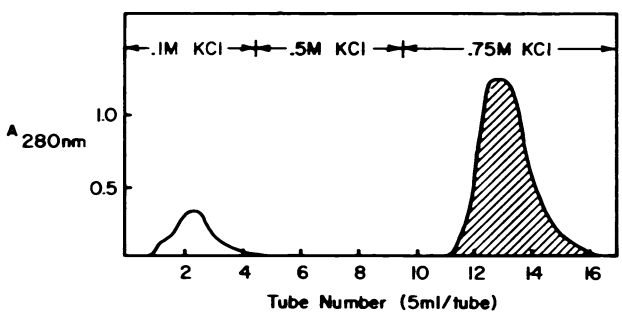

TEXT-FIGURE 2—Elution profile of fraction III (from G-50 column) on C-25 cation exchange column. The fraction was dissolved in elution buffer composed of 0.05 M Tris buffer (pH 9.0 at 21 C) and 0.1 M KCl and applied to the column. The column was equilibrated with elution buffer then developed with a stepwise KCl gradient in 0.05 M Tris buffer. *Hatched area* indicates fraction with myotoxic activity.

plasmalemma, external lamina, and nuclei were all typical of those found in normal skeletal muscle.

Experimental Muscle

Gross examination of experimental muscle revealed neither hemorrhage nor edema. Light microscopic examination still failed to reveal hemor rhage or edema, but focal areas of muscle degeneration were observed. The degree and extent of the damage varied directly with the amount of time elapsed between injection of the toxin and death of the animal. At 3 hours after injection no lesions were visible by light microscopy, but by 6 and 12 hours small vacuoles could be seen in portions of some muscle cells (Figure 4). By 24 hours after injection the vacuoles completely filled affected fibers, and up to one-half of the cells in a fascicle were vacuolated. The changes observed after 48 and 72 hours were similar to those seen at 24 hours except that, in addition to vacuolation, some fibers had lost their striated appearance (Figure 5). At no time was hemorrhage or hemolysis observed in these tissues.

Electron microscopic observation confirmed the results seen with the light microscope and revealed other changes. Intact muscle fibers were located next to damaged fibers, and the proportion of damaged fibers increased with the time after injection. The earliest observable signs of degeneration were dilatation of the sarcoplasmic reticulum (Figure 6) and perinuclear space (Figures 7 and 8). The typically flattened cisterns were swollen and much enlarged and became larger as degeneration progressed. Perinuclear space was greatly enlarged at one pole of the nucleus (Figures 7 and 8). The sarcoplasmic reticulum was enlarged, more disorganized, and occupied a larger portion of the cytoplasm at 24 hours after injection (Figures 9–10). Many of the dilatated cisterns contained myeloid figures (Figures 10 and 11).

Even though the cisterns of the sarcoplasmic reticulum were grossly enlarged, the transverse tubules (T tubule) retained their normal appearance (Figures 9–12). At 48 hours after injection of the component the cisterns had become smaller and fewer (Figure 13). The T tubules were still structurally intact (Figure 12). At this time there appeared to be some disintegration of muscle myofibrils (Figure 13). Also, mitochondria were slightly swollen and contained areas devoid of cristae, but severe mitochondrial damage was not seen even in areas where there was complete breakdown of the organization of myofibrils.

At 72 hours, portions of some fibers lacked the typical striated appearance. In these areas, intact sarcomeres were separated by loose actin and myosin filaments (Figures 14 and 15). Dissolution of the sarcomeres

occurred first between Z lines, and the Z-line material retained the longitudinal orientation of the myofilaments (Figures 14 and 15). In some areas the only recognizable remnant of the sarcomere was Z-line material (Figure 15). Intact T tubules were present in these areas (Figure 15).

Extreme mitochondrial degeneration was not observed even in areas where myofibrils were atrophied (Figures 14 and 15). In one instance, swelling of mitochondrial matrix was observed (Figure 13).

Other than dilatation of the perinuclear space (Figures 7 and 8), nuclear changes were not observed.

There was no structural damage to endothelial cells of capillaries, erythrocytes, or connective tissue cells (Figure 7).

Discussion

Since commercial antivenin prevents death due to snake envenomation, the major health problem resulting from snakebite in the United States is local tissue damage, i.e., hemorrhage and myonecrosis. The pathogenesis of hemorrhage [7] and myonecrosis [9] induced by crude rattlesnake venom has been studied at both the light and electron microscopic levels. Since crude venom contains a large number of components with different biologic actions, it is difficult to separate the pathologic effects of one component from those of another. This study clarifies the pathogenesis of snake venom–induced myonecrosis by using an isolated, purified myotoxic component of *Crotalus viridis viridis* venom.

Intramuscular injection of the pure myotoxic component into mice caused dilatation of the perinuclear space and sarcoplasmic reticulum with subsequent disruption of the myofibrils. The primary action of the toxin was on the sarcoplasmic reticulum. The structure of the sarcolemma and T-tubule system was not affected by the component.

Stringer *et al.*[9] reported similar results following injection of the crude venom except that they also observed hemorrhage, hemolysis, severe mitochondrial changes, and extensive disruption of the external lamina and sarcolemma. None of these changes was observed following injection of the pure component; thus, they were probably due to hemorrhagic and/or other components present in crude venom. The presence of hemorrhagic components has been demonstrated for several venoms,[16-19] and phospholipase A in venom acting on lecithin leads to production of lysolecithin which causes hemolysis.[20] Thus, myonecrosis induced by crude venom is complicated by the action of other factors.

Cobra venom causes local necrosis [21] without hemorrhage,[22] therefore, the pathogenesis of necrosis induced by this venom would not involve the action of hemorrhagic components. Stringer *et al.*[23] studied myonecrosis induced by cobra venom at the electron microscopic level and reported

coalesced myofilaments, swollen and lysed mitochondria, and a swollen and disrupted sarcotubular system. However, the initial effect did not appear to be on the sarcoplasmic reticulum as was the case with crude crotalid venom and the pure myotoxic component.

Tu *et al.*[24] and Homma and Tu [8] showed that venom from snakes of the families Crotalidae, Viperidae, and Elapidae caused myonecrosis observable with the light microscope. The type of necrosis varied between families and within a single family. Some venoms induced a coagulation type of myonecrosis (*C. viridis viridis*), some a myolytic type (all elapids), and some a mixed type (some crotalids). Thus, the pathogenesis of myonecrosis may differ depending on the type of snake venom used.

Myonecrosis induced by scorpion (*Tityus serrulatus*) venom [25] included dilatation of the sarcoplasmic reticulum and disorganization of myofilaments in a process very similar to that reported in this paper. Incubation of frog muscles in hornet (*Vespa orientalis*) venom [26] caused vacuolation of muscle fibers, as did the myotoxic component from rattlesnake venom. Hornet venom caused dilatation of T tubules as well as sarcoplasmic reticulum.

The differential expansion of intracellular membrane compartments as seen in Figures 6–15 is a common response of mammalian cells to injury.[27] This may be due to loss of cell volume control resulting from damage to the plasma membrane. In fact, endothelial cells responded to crude rattlesnake (*C. atrox*) venom in this way.[7] However, the isolated myotoxic component had no effect on endothelial cells, erythrocytes, or connective tissue cells. Therefore, it appears that the action of the component is somehow specific for skeletal muscle cells.

Since the sarcoplasmic reticulum serves as a calcium sink, it is possible that the pure component interferes with this function of the sarcoplasmic reticulum. Evidence for this comes from physiologic studies in which the contractile response of muscle was blocked by venom. An elapid (*Dendroaspis jamesoni*) venom completely prevented the contraction of frog sartorius muscle to indirect as well as direct stimulation.[28] That high calcium prevented these effects indicates damage to structure and function of the sarcoplasmic reticulum.

Studies which would correlate the physiologic and morphologic changes induced by pure myotoxic components are needed to further our understanding of myonecrosis induced by venom, as well as that occurring in many muscle diseases.

References

1. Swaroop, S, Grab, B: The snakebite mortality problem in the world. Venoms. Edited by EE Buckley, N Porges. Washington DC, American Association for the Advancement of Science, 1956

2. Parrish HM, Silberg SL, Goldner JC: Snakebite: A pediatric problem. Clin Pediatr 4:237–241, 1965
3. Vick JA: Symptomatology of experimental and clinical crotalid envenomation. Neuropoisons, Vol 1, Their Pathophysiological Actions. Edited by LL Simpson. New York, Plenum Press, 1971, pp 71–86
4. Minton SA Jr: Polyvalent antivenin in the treatment of experimental snake venom poisoning. Am J Trop Med Hyg 3:1077–1082, 1954
5. Stahnke HL, Allen FM, Horan RV, Tenery JH: The treatment of snake bite. Am J Trop Med Hyg 6:323–335, 1957
6. Homma M, Tu AT: Antivenin for the treatment of local tissue damage due to envenomation by Southeast Asian snakes: Ineffectiveness in the prevention of local tissue damage in mice after envenomation. Am J Trop Med Hyg 19:880–884, 1970
7. Ownby CL, Kainer RA, Tu AT: Pathogenesis of hemorrhage induced by rattlesnake venom: An electron microscopic study. Am J Pathol 76:401–414, 1974
8. Homma M, Tu AT: Morphology of local tissue damage in experimental snake envenomation. Br J Exp Pathol 52:538–542, 1971
9. Stringer JM, Kainer RA, Tu AT: Myonecrosis induced by rattlesnake venom: An electron microscopic study Am J Pathol 67:127–140, 1972
10. Okonogi T, Homma M, Hoshi S: Pathological studies on habu-snake bite. Gunma J Med Sci 13:101–120, 1964
11. Lowry OH, Rosenbrough NJ, Farr AL, Randall RJ: Protein measurement with the Folin phenol reagent. J Biol Chem 193:265–275, 1951
12. Jovin TM, Dante ML, Chrombach A: Unpublished data
13. Lockwood WR: A reliable and easily sectioned epoxy embedding medium. Anat Rec 150:129–132, 1964
14. Lynn JA: Rapid toluidine blue staining of Epon-embedded and mounted "adjacent" sections. Am J Clin Pathol 44:57–58, 1956
15. Venable JH, Coggeshall R: A simplified lead citrate stain for use in electron microscopy. J Cell Biol 25:407–408, 1965
16. Ohsaka A, Ikezawa H, Kondo H, Kondo S: Two hemorrhagic principles derived from Habu snake venom and their difference in zone electrophoretical mobility. Jap J Med Sci Biol 13:73–76, 1960
17. Satake M, Murata Y, Suzuki T: Studies on snake venom. XIII. Chromatographic separation and properties of three proteinases from *Agkistrodon halys blomhoffii* venom. J Biochem 53:438–447, 1963
18. Omori T, Iwanaga S, Suzuki T: The relationship between the hemorrhagic and lethal activities of Japanese Mamushi (Agkistrodon halys Blomhoffii) venom. Toxicon 2:1–4, 1964
19. Grotto L, Moroz C, De Vries A, Goldblum N: Isolation of *Vipera palestinae* hemorrhagin and distinction between its hemorrhagic and proteolytic activities. Biochim Biophys Acta 133:356–362, 1967
20. Leven PA, Rolf IP: Lysolecithins and lysocephalins. J Biol Chem 60:743–749, 1923
21. Reid HA: Cobra-bites. Br Med J 2:540–545, 1964
22. Tu AT, Toom PM, Ganthavorn S: Hemorrhagic and proteolytic activities of Thailand snake venoms. Biochem Pharmacol 16:2125–2130, 1967
23. Stringer JM, Kainer RA, Tu AT: Ultrastructural studies of myonecrosis induced by cobra venom in mice. Toxicol Appl Pharmacol 18:442–450, 1971
24. Tu AT, Homma M, Hong BS: Hemorrhagic, myonecrotic, thrombotic and proteolytic activities of viper venoms. Toxicon 6:175–178, 1969
25. Rossi MA, Ferreira AL, Paiva SM, Santos JCM: Myonecrosis induced by scorpion venom. Experientia 29:1272–1274, 1973
26. Ishay J, Lass Y, Sandbank U: A lesion of muscle transverse tubular system by oriental hornet (*Vespa orientalis*) venom: Electron microscopic and histological study. Toxicon 13:57–59, 1975

27. Ginn FL, Shelburne JD, Trump BF: Disorders of cell volume regulation. I. Effects of inhibition of plasma membrane adenosine triphosphatase with ouabain. Am J Pathol 53:1041–1071, 1968
28. Patel R, Excell BJ: The modes of action of whole *Dendroaspis jamesoni* venom on skeletal nerve-muscle preparations. Toxicon 12:577–585, 1974

Acknowledgments

The authors would like to thank K. Kocan for sectioning the material and D. Collins for typing the manuscript.

[*Illustrations follow*]

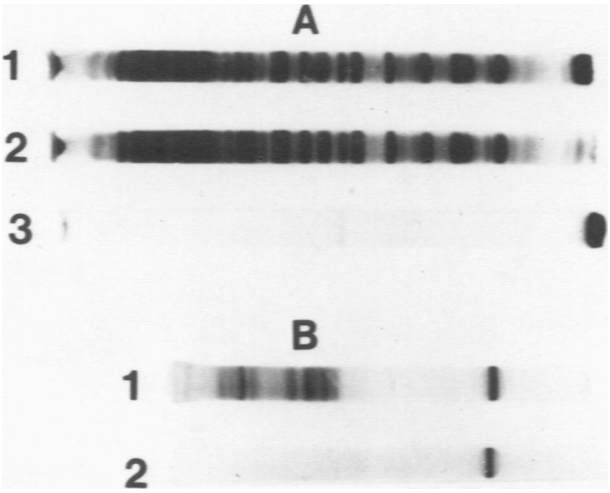

Figure 1—Results of polyacrylamide gel electrophoresis. **A**—Isoelectric focusing gels, pH range 3.5 to 10, from left to right; *Gel 1,* 150 μg crude venom, gel soaked in 20% TCA containing 10 mM $HgCl_2$ prior to staining. *Gel 2,* 150 μg crude venom, gel soaked in 20% TCA prior to staining. *Gel 3,* 40 μg fraction C-25 II, gel soaked in 20% TCA containing 10 mM $HgCl_2$ prior to staining. **B**—β-Alanine disc gels, top of gels on the left. *Gel 1,* 100 μg crude venom. *Gel 2,* 25 μg fraction C-25 II.

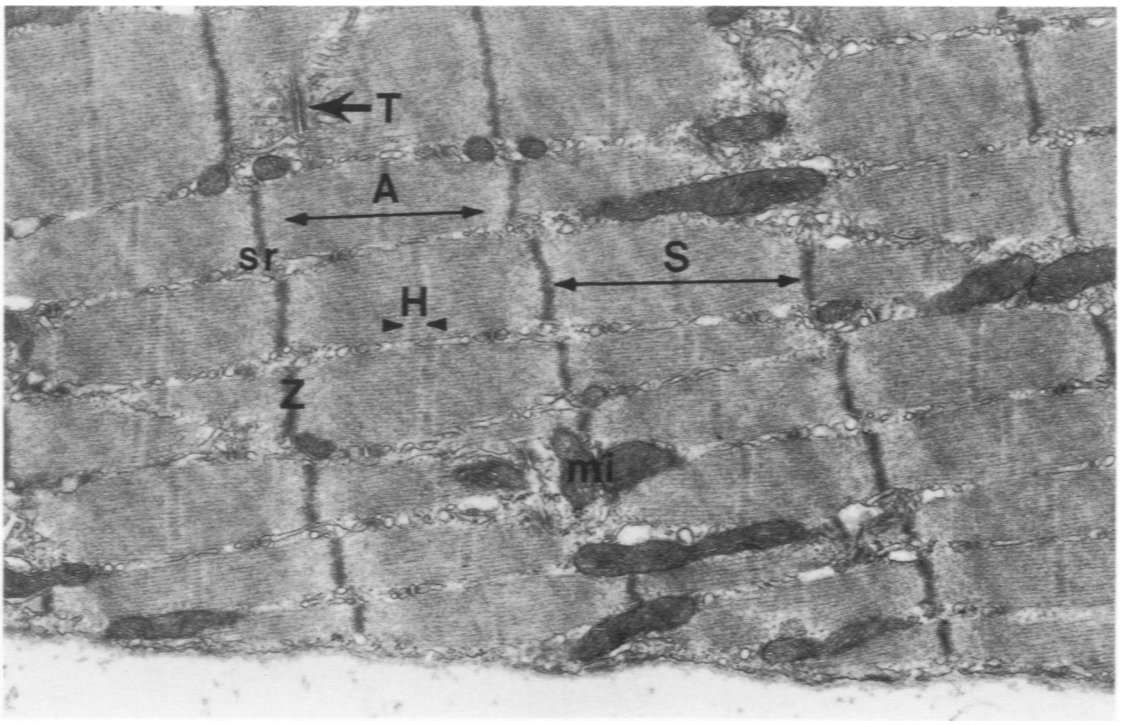

2

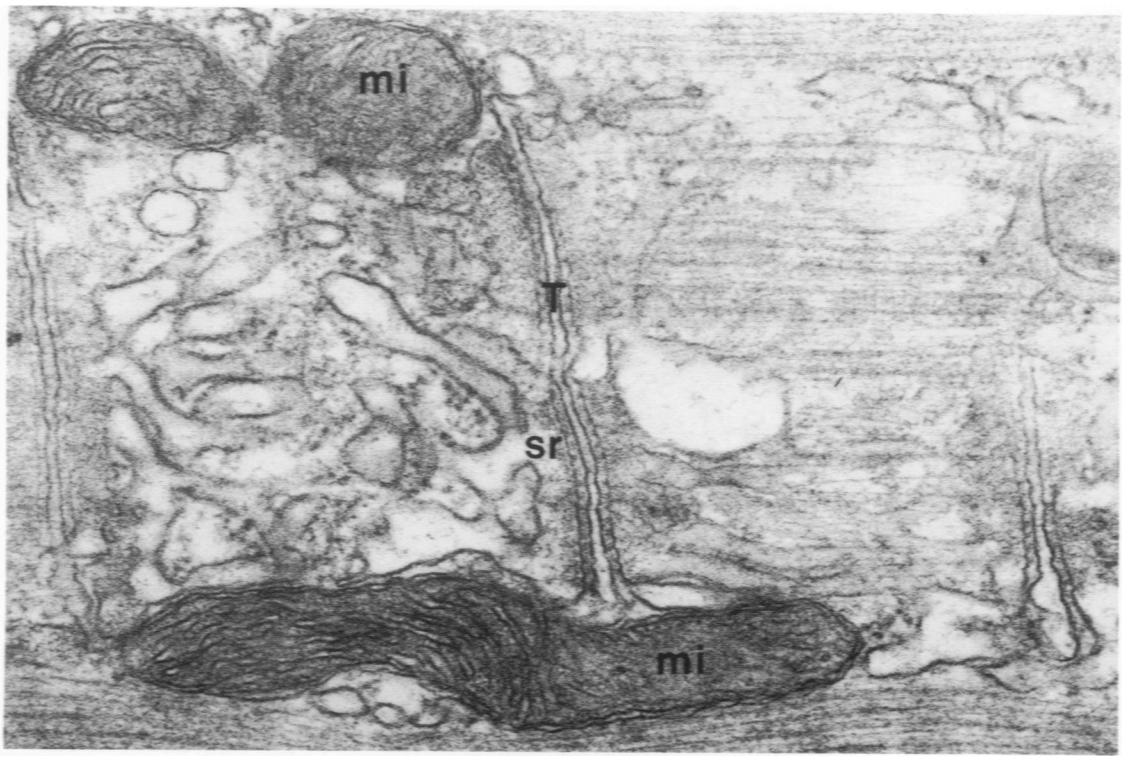

3

Figure 2—Electron micrograph of muscle from control animal. *Z* = Z line, *S* = sarcomere, *A* = A band, *H* = H band, *sr* = sarcoplasmic reticulum, *T* = T tubule, *mi* = mitochondria. (×17,000) **Figure 3**—High magnification electron micrograph showing triad of control muscle. *T* = T tubule, *sr* = sarcoplasmic reticulum, *mi* = mitochondria. (×63,000)

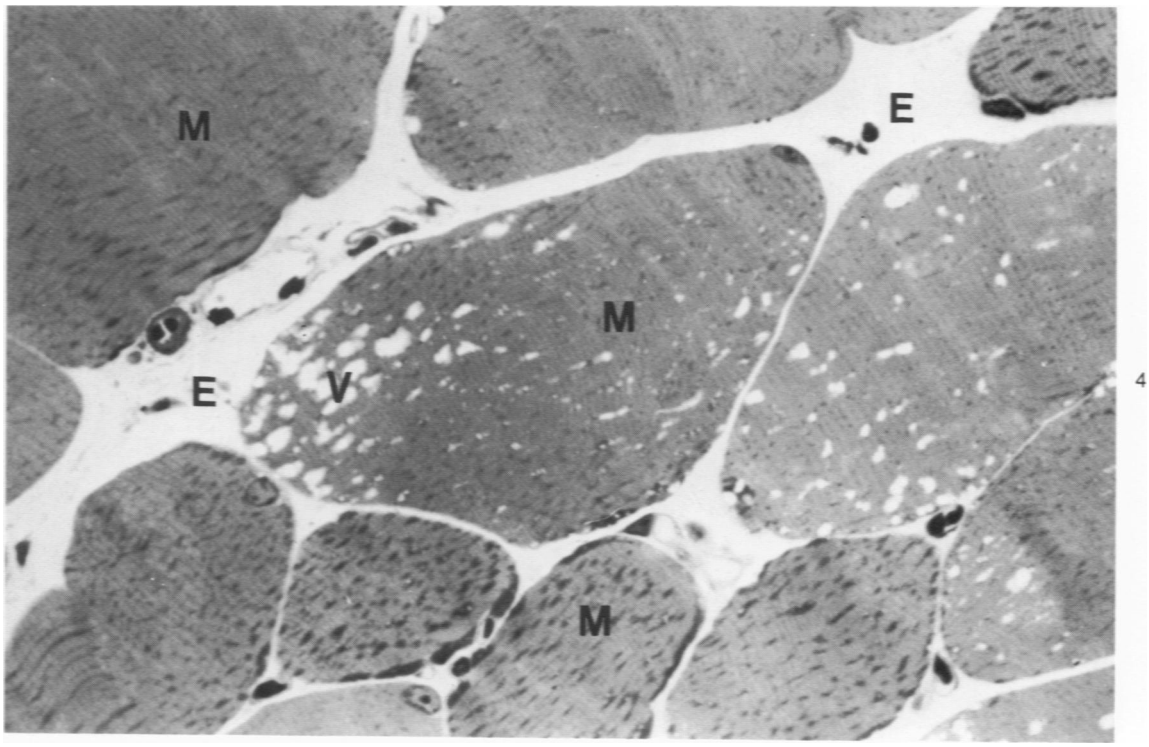

4

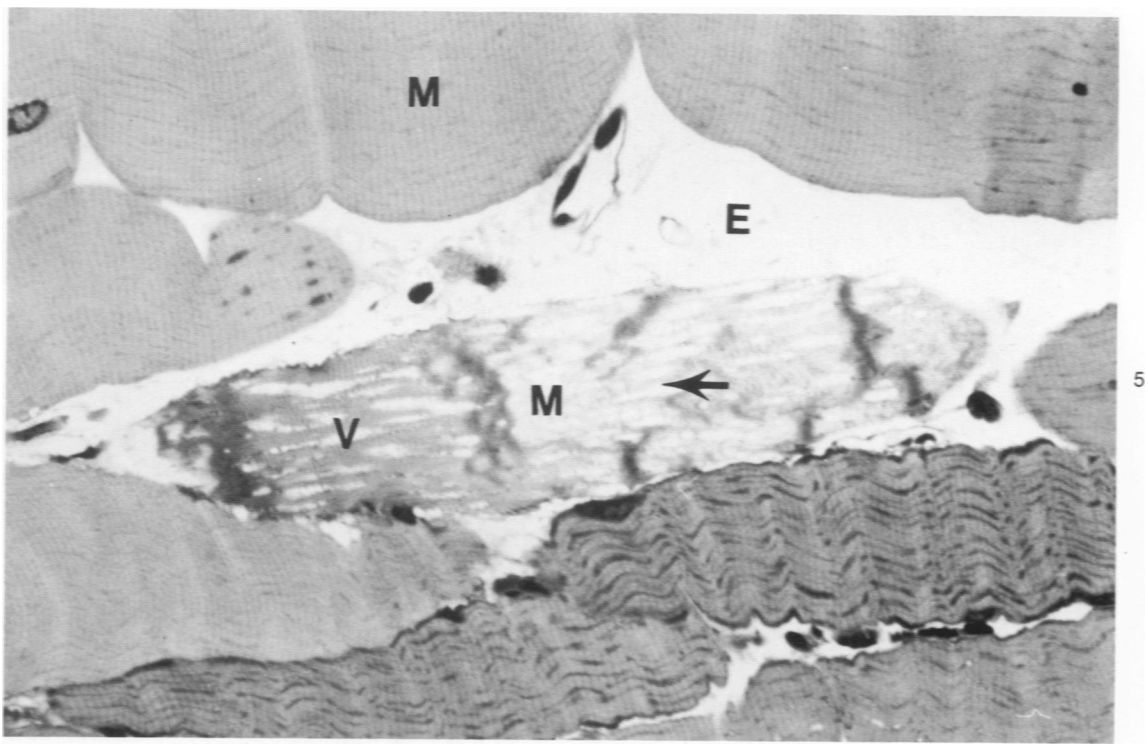

5

Figure 4—Light micrograph of muscle 12 hours postinjection. *M* = muscle fibers, *E* = endomysium. Note numerous vacuoles (*V*) in damaged fibers and absence of hemorrhage in endomysium. (Original magnification ×200) **Figure 5**—Light micrograph of muscle 72 hours postinjection. *M* = muscle cells, *E* = endomysium. Note degenerating fiber which contains some vacuoles (*V*) and has lost striated appearance (*arrow*). (×200)

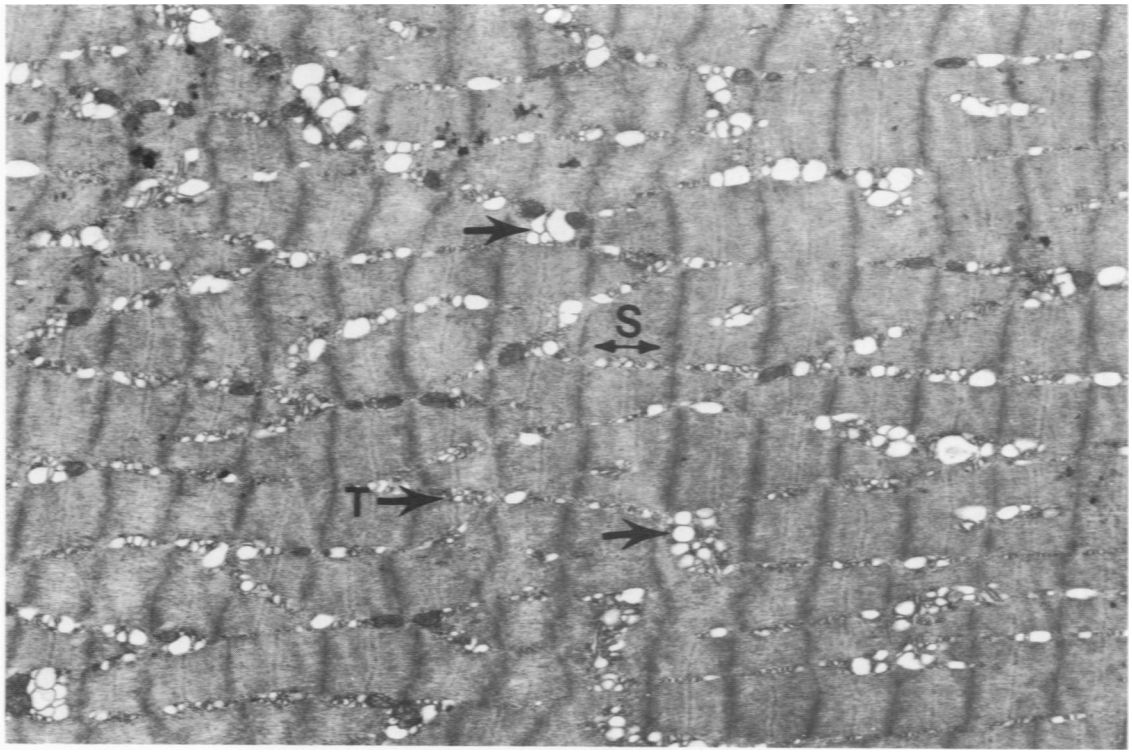

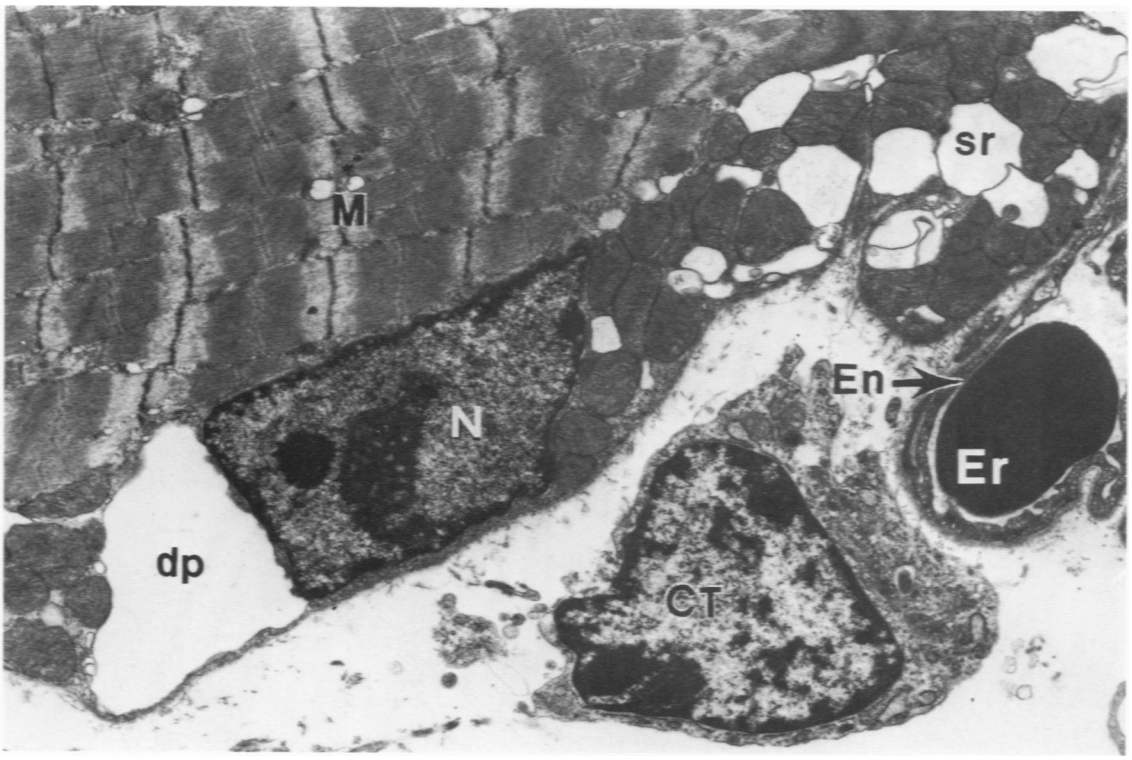

Figure 6—Muscle 3 hours postinjection. Note dilatation of sarcoplasmic reticulum (*arrows*). Sarcomeres (*S*) and T tubules (*T*) are intact. (×9000) **Figure 7**—Muscle 12 hours postinjection. *M* = muscle fiber, *N* = nucleus of muscle cell, *CT* = connective tissue cell, *En* = endothelial cell of capillary, *Er* = erthrocyte. Note dilatated perinuclear space (*dp*) and dilatated sarcoplasmic reticulum (*sr*). Connective tissue cell, capillary and erythrocyte are all structurally intact. (×8500)

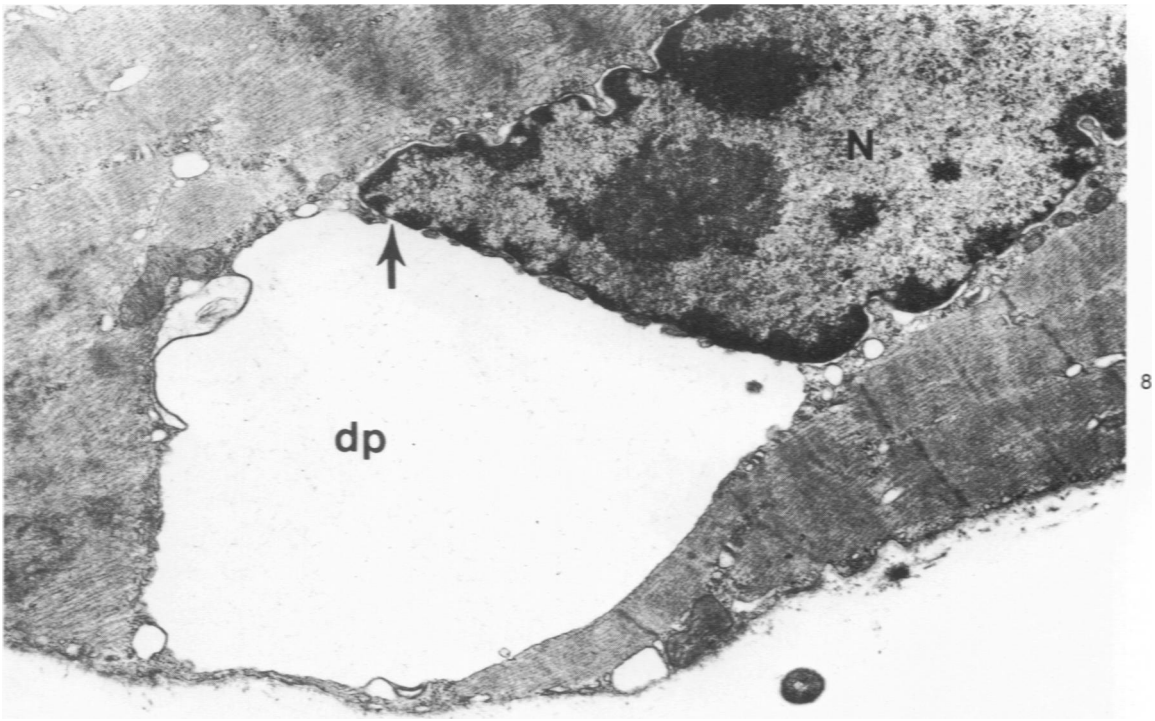

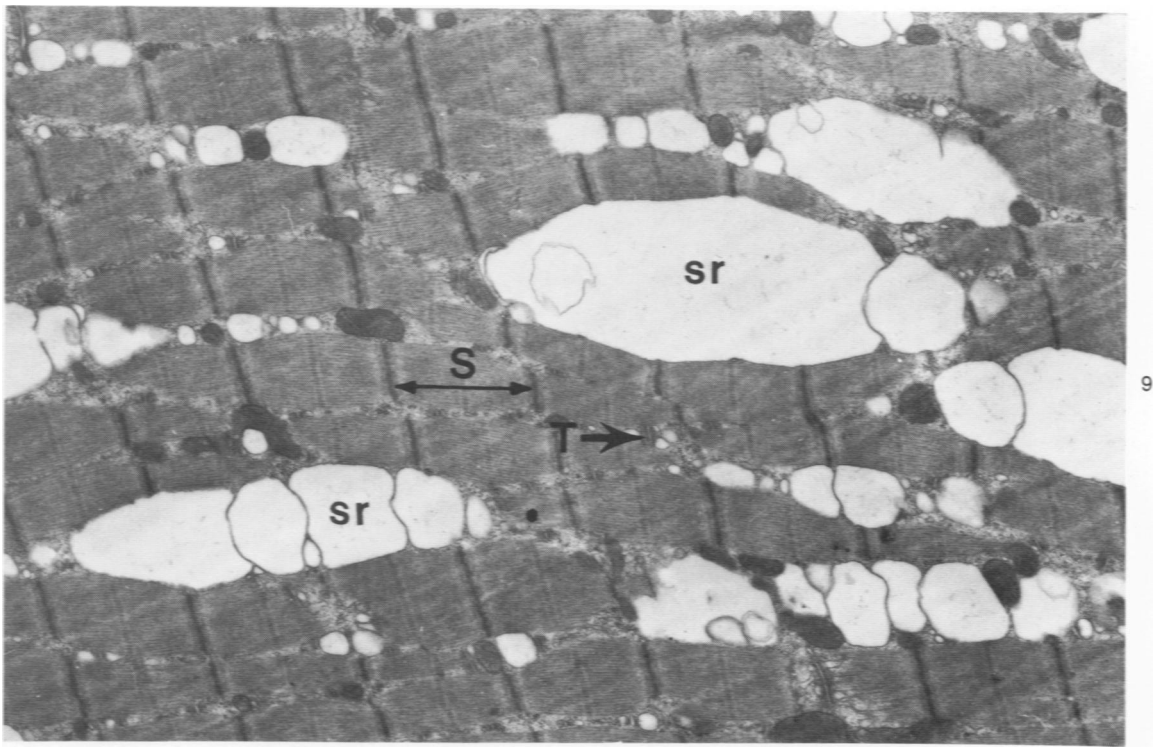

Figure 8—Muscle 12 hours postinjection. High magnification of muscle cell showing nucleus (*N*) and dilatated perinuclear space (*dp*). Note continuity of dilatated portion with nondilatated portion (*arrow*). (×15,500) **Figure 9**—Muscle 12 hours postinjection. Sarcoplasmic reticulum is greatly dilatated (*sr*), but sarcomeres (*S*) and T tubules (*T*) are not altered. (×12,000)

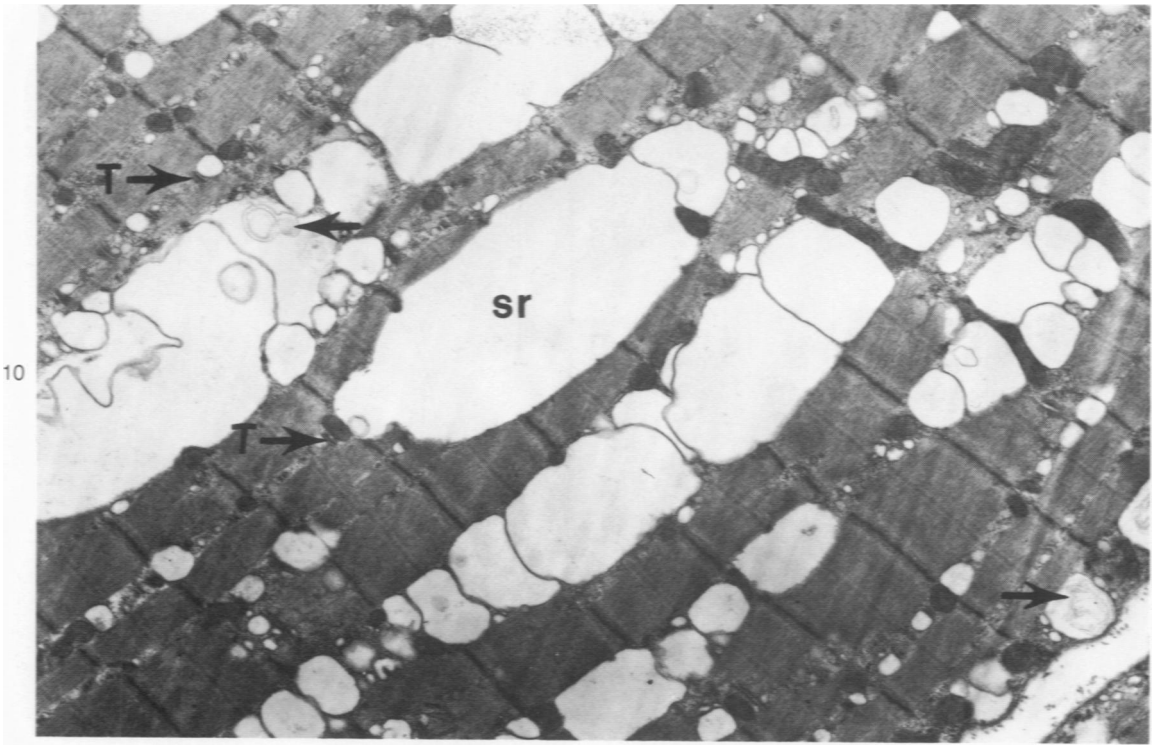

10

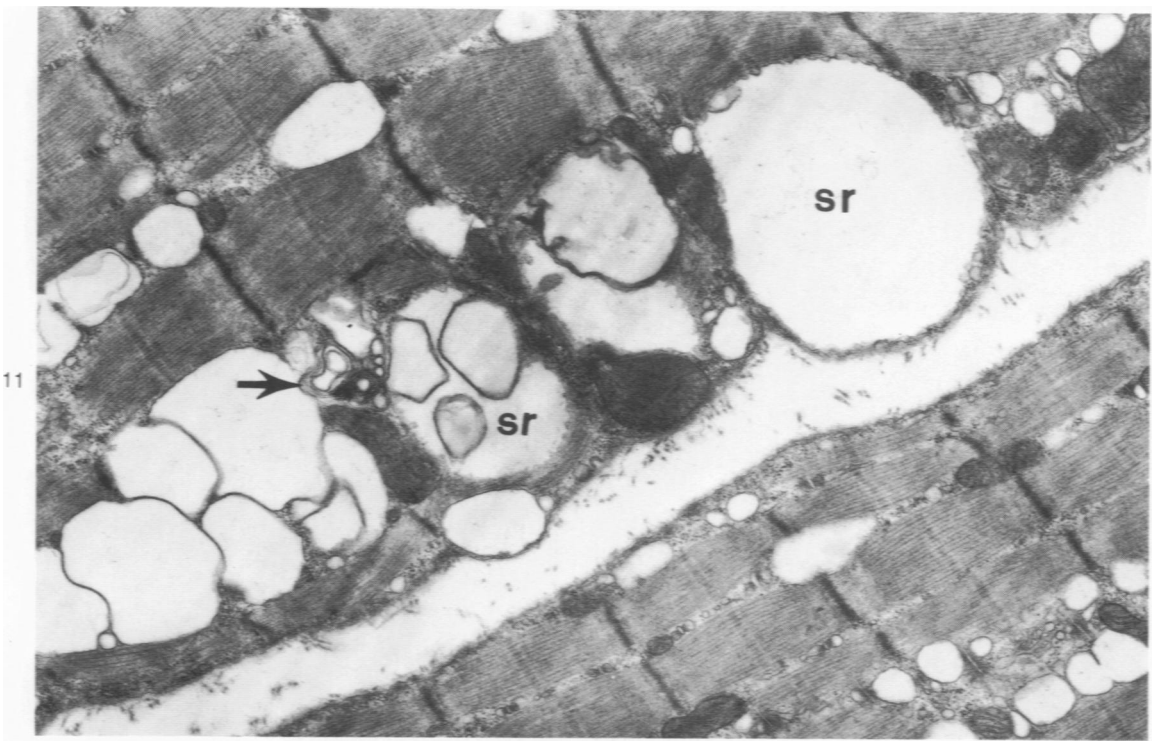

11

Figure 10—Muscle 24 hours postinjection. Sarcoplasmic reticulum is greatly dilatated (*sr*), but T tubules (*T*) are not altered. Myeloid figures are present (*arrows*). (×13,000) **Figure 11**—Muscle 24 hours postinjection. Higher magnification of area showing dilatated sarcoplasmic reticulum (*sr*) and myeloid figure (*arrow*). (×16,000)

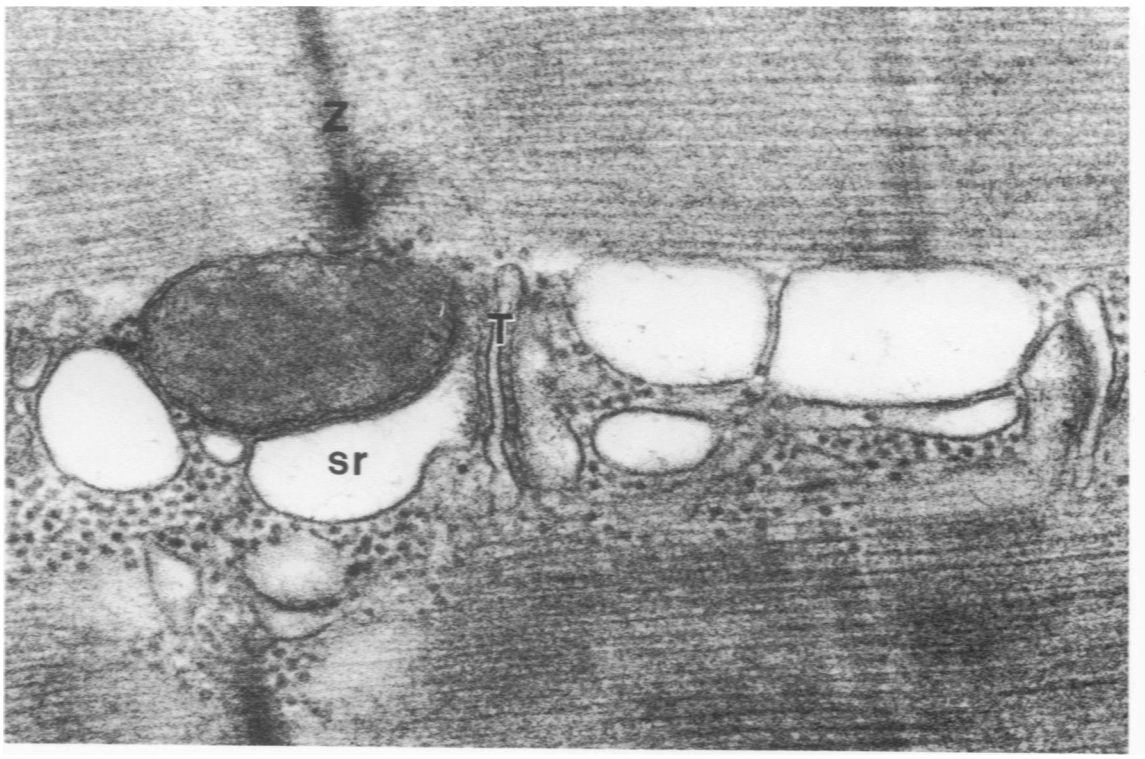

12

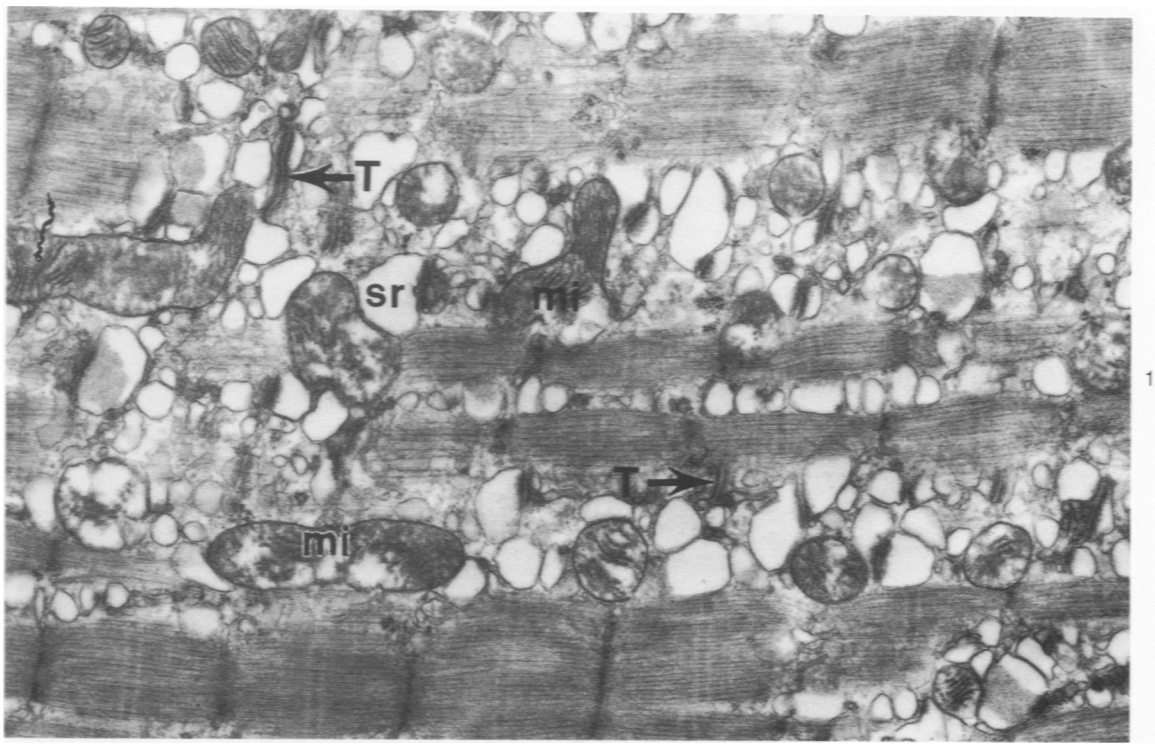

13

Figure 12—Muscle 24 hours postinjection. The high magnification shows the intactness of T tubule (*T*) and that the sarcoplasmic reticulum (*sr*) is dilatated. *Z* = line. (×76,000) **Figure 13**—Muscle 48 hours postinjection. Note numerous smaller dilatated cisterns of sarcoplasmic reticulum (*sr*). T tubules (*T*) remain intact, but some mitochondria are swollen (*mi*). (×17,000)

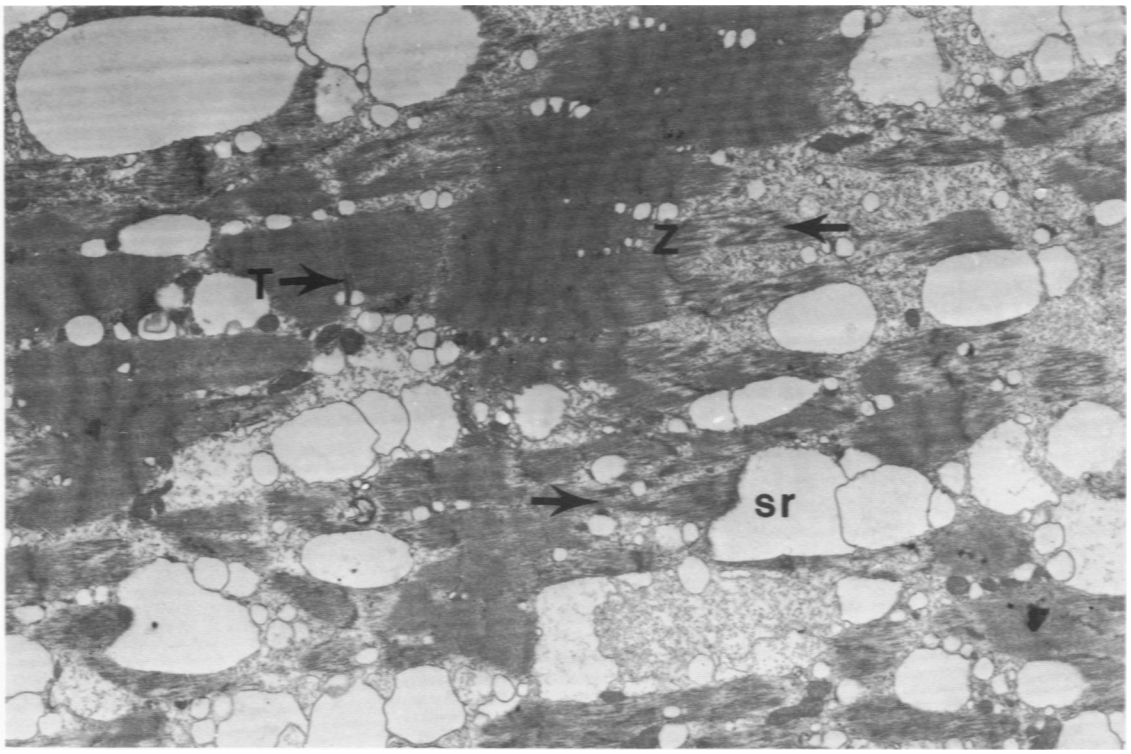

14

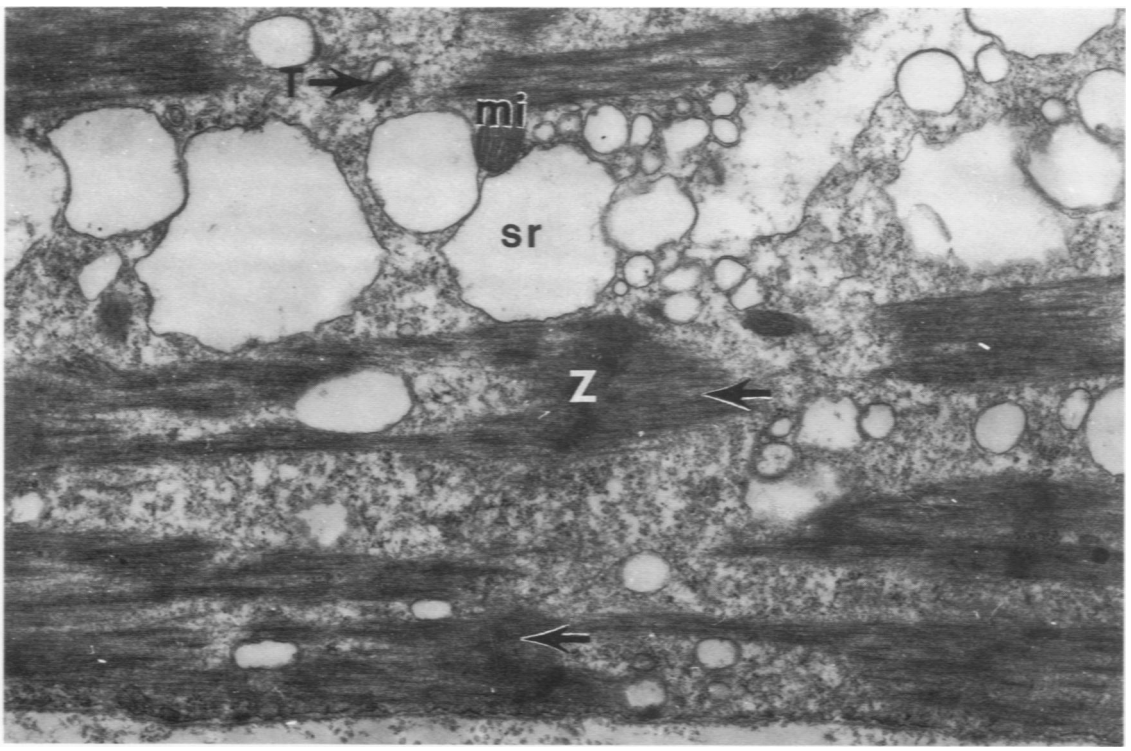

15

Figure 14—Muscle 72 hours postinjection. Myofibrils are degenerating (*arrows*). *Sr* = dilatated sarcoplasmic reticulum, *Z* = Z lines, *T* = intact T tubule. (×10,000)

Figure 15—Muscle 72 hours postinjection. Note the degenerating myofibrils (*arrows*). *Z* = Z-line material, *sr* = dilatated sarcoplasmic reticulum, *T* = intact T tubule, *mi* = mitochondrion. (×22,500)